Electrochemical Polymerization and Characterization of Poly(3-(4-fluorophenyl)thiophene) in Pure Ionic Liquids

Eric Naudin,[†] Hoang Anh Ho,[‡] Stéphane Branchaud,[‡] Livain Breau,*[,‡] and Daniel Bélanger*[,†]

Département de Chimie, Université du Québec à Montréal, Case Postale 8888, succursale Centre-Ville, Montréal (Québec) Canada H3C 3P8, and Laboratoire de Synthèse Organique Appliquée, Département de Chimie, Université du Québec à Montréal, Case Postale 8888, succursale Centre-Ville, Montréal (Québec) Canada H3C 3P8

Received: March 20, 2002; In Final Form: June 28, 2002

The electrochemical oxidation of 3-(4-fluorophenyl) thiophene (FPT) at a platinum electrode in pure 1-ethyl-2,3-dimethylimidazolium bis ((trifluoromethyl)sulfonyl) amide, EDMITFSI, and 1,3-diethyl-5-methylimidazolium bis ((trifluoromethyl)sulfonyl) amide, DEMITFSI, yielded an electroactive polymer. This polymer (PFPT) was similar to that prepared from common nonaqueous media such as tetraethylammonium tetrafluoroborate/acetonitrile, but it was characterized by slower ion insertion kinetics. A rapid loss of electroactivity of the polymer was observed upon cycling in pure ionic liquid, and that was attributed to gradual deswelling of the polymer. X-ray photoelectron spectroscopy measurements demonstrated that the doping processes of PFPT when cycled in pure ionic liquid were similar to those occurring in acetonitrile-based electrolyte and involved the incorporation of the anions ($TFSI^-$) of the ionic liquid when the polymer was oxidized to the p-doped state. The expulsion of these anions and the incorporation of the ionic liquid cationic species were observed upon reduction of the polymer to the fully n-doped state.

Introduction

Conducting polymers are currently attracting significant interest worldwide because of their potential applications in energy storage devices, electrochromic devices, and light emitting diodes.[1,2] These polymers were prepared either by chemical or electrochemical polymerization. The electrochemical synthesis offers several advantages, including rapidity, simplicity, generation of the polymer in the doped state and easy control of the amount (film thickness) generated.[3] Despite these advantages, some drawbacks limit the application of this approach to all monomers. For instance, the monomer might be insoluble in the solvent or the resulting polymer is soluble rather than being generated at the electrode surface. Of course, the later is critical if one objective is to grow a polymer on the electrode surface. Solvents such as water and acetonitrile have been commonly used for the electropolymerization of conjugated polymers.[1] On the other hand, these polymers have been also grown from less common media such as liquid ammonia[4] and chloroaluminate melts.[5,6]

Room-temperature ionic liquids are becoming a solvent of choice for several chemical applications as they can replace classic organic solvents which may be too volatile and/or hazardous.[7−16] For example, they can be used as solvents for industrially important organic reactions such as regioselective alkylation,[12] Friedal−Crafts acetylations,[13] and biphasic hydrogenation.[14] Ionic liquids are also able media for the development of novel liquid−liquid extraction processes.[7] In addition, a new class of ionic liquids comprising substituted imidazolium cations and the bis[(trifluoromethyl)sulfonyl)]amide anion (Scheme 1; in place of the air unstable and undesirable $AlCl_4^-$anions) have been recently investigated for applications in various electrochemical systems because they are stable over a wide potential window.[15,16] Thus, ionic liquids may become solvents of choice for the electrochemical generation of conjugated polymers. As mentionned above, polypyrrole can be electrochemically grown from a pyrrole, $AlCl_3$/N-1-butylpyridinium (or $AlCl_3$/1-methyl-(3-ethyl-imidazolium chloride), solution.[5,6]

SCHEME 1: Structure of the Ionic Liquids. A. 1-Ethyl-2,3-dimethylimidazolium bis ((trifluoromethyl)sulfonyl) amide, EDMITFSI. B. 1,3-Diethyl-5-methylimidazolium bis ((trifluoromethyl)sulfonyl) amide, DEMITFSI

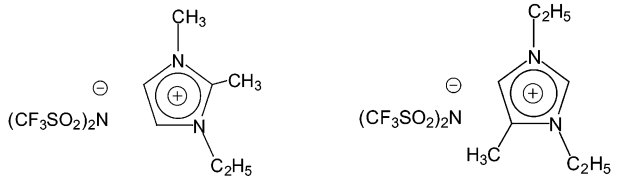

In this paper, we wish to demonstrate the usefulness of two pure ionic liquids, 1-ethyl-2,3-dimethylimidazolium bis((trifluoromethyl)sulfonyl) amide, EDMITFSI, and 1,3-diethyl-5-methylimidazolium bis ((trifluoromethyl)sulfonyl) amide, DEMITFSI, as solvent and electrolyte with conducting polymer electrode such as poly(3-(4-fluorophenyl) thiophene) (PFPT). The latter has been studied in great detail in conventional nonaqueous media based on acetonitrile as solvent.[17−25] In this work, the electropolymerization of PFPT in the aforementioned ionic liquids was investigated with the aim of determining the effect of the ionic liquid on the electropolymerization process. Some effect might be anticipated because the electropolymerization process involves an electrogenerated cation radical as the reactive species and that several species (ions and solvent)

* To whom correspondence should be addressed. E-mail: breau.livain@uqam.ca. E-mail: belanger.daniel@uqam.ca.

[†] Département de Chimie, Université du Québec à Montréal.

[‡] Laboratoire de Synthèse Organique Appliquée, Département de Chimie, Université du Québec à Montréal.

10.1021/jp020770s CCC: $22.00
Published on Web 09/20/2002

might promote or interfere with the polymerization process. The resulting polymer was characterized by cyclic voltammetry and electrochemical impedance spectroscopy. Finally, the ionic transport upon redox switching between the p- and n-doped states in pure ionic liquid was investigated by means of X-ray photoelectron spectroscopy.

Experimental Section

Chemicals. The synthesis of FPT,[21] EDMITFSI,[15,26] and DEMITFSI[15,26] have been performed according to published procedures. Acetonitrile (HPLC grade) from Aldrich was used without further purification. Tetraethylammonium tetrafluoroborate (Et_4NBF_4) (Aldrich, 99%) was recrystallized three times from methanol and dried under vacuum at 140 °C for 12 h prior to use.

Materials. A platinum disk (diameter = 1 mm) sealed inside a glass tube or epoxy and a platinum grid (area = 1 cm^2) were used as working and counter electrodes, respectively. The reference electrode was Ag/Ag^+ (10 mM $AgNO_3$, 0.1 M tetrabutylammonium perchlorate in acetonitrile). The electrode assembly for the in situ conductivity measurements consists of two platinum band electrodes (3×0.12 mm for each band) with interband spacing of 60 μm (Mylar films, Dupont) to be bridged by the deposited material.[27−30] The electrodes were polished with 0.05 μm alumina slurry (Buehler) and washed with water and cleaned ultrasonically before use.

Procedure and Electrochemical Measurements. All electrochemical measurements were performed in a glovebox under a dry and N_2 atmosphere, in a closed three-electrode cell. Electrochemical impedance spectroscopy data were collected at various electrode potentials over a frequency range of 65 kHz to 0.05 Hz using a 10 mV (rms) amplitude sine wave. The polymer electrode was polarized at the appropriate potential for about 60 s before the impedance measurements were taken in order to ensure that the polymer film electrode had reached equilibrium.

X-ray Photoelectron Spectroscopy, XPS. For the XPS measurements, the polymers were removed from either the monomer/ionic liquid solution (for the as-grown polymer) or the pure ionic liquid (p- and n-doped) and rinsed thoroughly with CH_2Cl_2. It is essential to rinse the polymer with this solvent because of the viscous nature and low vapor pressure of the ionic liquid that remained at the electrode surface when an XPS spectrum of the ionic liquid is recorded. Initial attempts to rinse the polymer with acetonitrile were unsuccessful as a significant amount of ionic liquid was detected by XPS as some remained at the polymer surface. The XPS data were obtained at room temperature and typically the operating pressure in the analysis chamber was below 1×10^{-9} Torr. XPS spectra were recorded for various PFPT film-coated platinum electrodes after being freshly electrodeposited (as-grown), reduced at − 2.07 V, and oxidized at 0.8 V in pure ionic liquid. Survey scans in the range of 0−1100 eV were recorded at a pass energy of 100 eV with a step size of 1 eV. Core level spectra were obtained for C 1s, S 2p, F 1s, and N 1s with a pass energy of 20 eV and a step size of 50 meV. Typically, one to four detailed scans were recorded. Curve fitting of the XPS data was carried out with Origin software (version 6.0). A semiquantitative evaluation of relative atomic surface concentrations was obtained by considering their corresponding sensitivity factors: C 1s (1.0), S $2p_{1/2}$ (0.567), S $2p_{3/2}$ (1.11), F 1s (4.43), and N 1s (1.8). The binding energies were corrected for surface charging by referencing them to the designated hydrocarbon C 1s binding energy at 284.5 eV. Although, the deconvolution of the XPS core level spectra is not straigthforward, it could be performed with good confidence by considering that $TFSI^-$ has a contribution to the N 1s, S 2p, and F 1s spectra. Thus, it is possible to evaluate the contribution of the residual ionic liquid and consequently the ionic content (as dopant ions) of the p- and n-doped PFPT.

Electropolymerization and Electrochemical Characterization. The polymer films were grown on a platinum electrode from a solution containing 0.17 M FPT in pure EDMITFSI (or DEMITFSI) ionic liquid and 0.17 M FPT in 1 M tetraethylammonium tetrafluoroborate in acetonitrile. The electropolymerization was performed galvanostatically at current densities of 1−12.7 mA/cm^2. The films were then washed (with pure ionic liquid or acetonitrile) in order to remove any soluble species from the film and cycled in a monomer free solution of a pure ionic liquid or 1 M tetraethylammonium tetrafluoroborate in acetonitrile.

The in situ conductivity measurements were performed by measuring the drain current, I_D, flowing between the two Pt band electrodes when a drain voltage of 25 mV is applied between them and at various electrode potentials by scanning the potential at 5 mV/s. Because the geometry (distance between electrodes and film thickness) is not very well characterized, only the I_D-potential curves are reported.

Equipment. Cyclic voltammetric studies were performed using a potentiostat (model 1287 Solartron Electrochemical Interface) coupled to a PC with Corrware Software for Windows (Scribner Associates, version 2.1b). Electrochemical impedance measurements were performed with a model 1255 Solartron Frequency Response Analyzer coupled to a model 1287 Solartron Electrochemical Interface. Data were collected and analyzed using a PC and Zplot Software for Windows (Scribner Associates, version 2.1b). XPS measurements were performed with a VG Escalab 220i-XL system equipped with an hemispherical analyzer and an Al anode (Kα X-rays at 1486.6 eV) at 10 kV and approximately 15 mA. The morphology of the deposited films was observed by SEM using a Hitachi model S-5300 microscope.

Results and Discussion

Electrochemical Polymerization. Figure 1 shows the cyclic voltammograms at a scan rate of 100 mV/s for a platinum electrode in a 0.17 M FPT solution in pure ionic liquid (EDMITFSI). The first cycle is characterized by an irreversible anodic and a cathodic wave at 1.28 and 0.42 V, respectively. The anodic wave is attributed to the oxidation of FPT to its cation radical. Alternately, PFPT can be deposited galvanostatically from the same solution or with other ionic liquid (DEMITFSI) as solvent. When PFPT was deposited at current density 12.7 mA/cm^2, a constant potential of 1.16 and 1.22 V was maintained during polymer formation in EDMITFSI and DEMITFSI, respectively (Table 1). The oxidation of FPT in ionic liquid occurs at a more positive potential relative to other solvents (propylene carbonate and acetonitrile) containing electrolytes salt such tetraethylammonium tetrafluoroborate and tetraethyammonium trifluoromethanesulfonate.[20,22] For instance, polymerization potentials of 0.98 V[20] and 1.1 V[22] have been reported for FPT in propylene carbonate and acetonitrile, respectively. The higher oxidation potential in ionic liquids reflects the fact that the cation radical is much less stabilized in these media. Clearly, the solvent (acetonitrile and propylene carbonate) can play a significant role in the stabilization of the cation radical, and these observations suggest that different polymers may be grown from acetonitrile and pure ionic liquid media. The cathodic wave at 0.42 V on the first scan refers to

TABLE 1: Voltammetric Cyclic Data for FPT and PFPT in Pure Ionic Liquids and 1 M Et_4NBF_4/Acetonitrile[a]

electrolyte (V)	Epa (V)	Egal (V)	Ep^+/p^- (V)	En+/n-	Qn^+/Qn^- (mC/cm^2)	Qp^+/Qp^- (mC/cm^2)	xp/xn
EDMITFSI	1.28	1.16	0.77/0.36	−2.1/-1.74	17.2/10.4	28.1/27.9	0.33/0.11
DEMITFSI	1.29	1.22	0.88/0.55	−2.02/-1.7	3.3/16.2	10.3/15.7	0.11/0.18
1 M Et_4NBF_4/ACN			0.71/0.62	−2.01/-1.93	17.1/23.7	23.7/16.5	0.27/0.27

[a] Epa: Anodic peak potential at a platinum electrode for a 0.17 M FPT + electrolyte solution at a scan rate of 100 mV/s. Egal: Stabilization potential during galvanostatic deposition at 12.7 mA/cm^2 at a platinum electrode from a 0.17 M FPT + electrolyte solution. Ep^+: Anodic potential peak for p doping. Ep^-: Cathodic potential peak for p doping. En^+: Anodic potential peak for n doping. En^-: Cathodic potential peak for n doping. Qp^+: Charge of the anodic wave for p doping. Qp^-: Charge of the cathodic wave for p doping. Qn^+: Charge of the anodic wave for n doping. Qn^-: Charge of the cathodic wave for n doping. xp: Doping level for p doping. xn: Doping level for n doping.

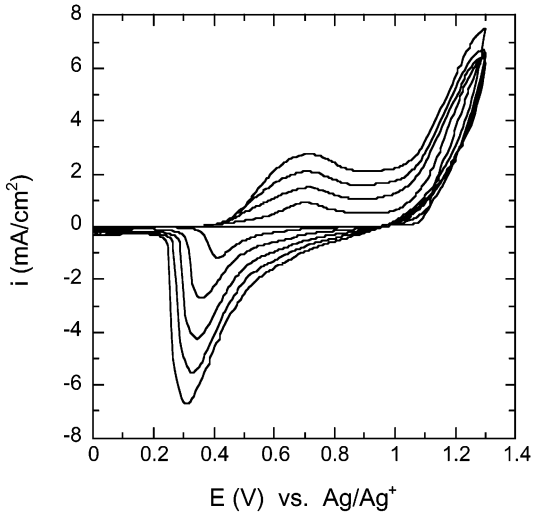

Figure 1. Cyclic voltammograms during electropolymerization for a platinum electrode in 0.17 M 3-(4-fluorophenyl)thiophene (FPT) in pure EDMITFSI ionic liquid. Scan rate = 100 mV/s

the reduction of polymer being deposited at the electrode surface on the forward scan. On subsequent scans, the increase of both the anodic (0.70 V) and cathodic (0.31 V) waves confirms the growth of polymer at the electrode surface. A significant peak potential separation is noticeable between the anodic and cathodic peak upon polymer growth and this feature will be discussed below.

Scanning Electron Microscopy, SEM. Photomicrographs of PFPT grown in the presence of the two ionic liquids are shown in Figure 2. Both films appear fairly smooth, and clearly, the polymer is not very porous, even at a magnification of 10 000. This might be a drawback for use of such PFPT as electrode material that typically involves movement of ions in and out of the polymer during redox switching. This aspect will be discussed further below. The smooth surface might indicate that a thin ionic liquid layer remained at the polymer surface as it will be confirmed later by XPS measurements.

Cyclic Voltammetry of PFPT. Figure 3 (curve − − −) depicts the cyclic voltammogram of PFPT ($Q_{deposited}$ = 200 mC/cm^2) in pure EDMITFSI ionic liquid at a scan rate of 100 mV/s. It is characterized by two sets of redox waves centered at about 0.56 V for p-doping and at −1.92 V for n-doping. The data of Table 1 suggest that the kinetics of the redox processes for a PFPT film electrode grown from a pure ionic liquid solution are more sluggish in an ionic liquid relative to an electrolyte such as Et_4NBF_4/acetonitrile. This is evidenced by the larger anodic and cathodic peak potential separation for the p-doping and p-dedoping waves of 0.41 V in EDMITFSI ionic liquid compared to 0.09 V in Et_4NBF_4/acetonitrile. A similar trend can be observed for the n-doping redox waves. The uncompensated solution resistance (iR_u) contributes also to the larger potential peak separation found in the presence of the

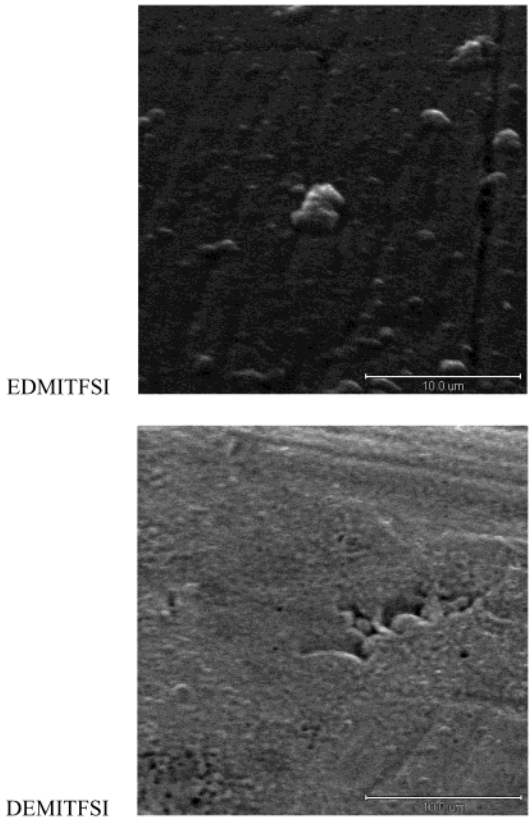

Figure 2. Photomicrograph of PFPT grown at a current density of 12.7 mA/cm^2 for a charge of 200 mC/cm^2 at the surface of a platinum foil electrode in (a) 0.17 M FPT and pure DEMITFSI and (b) 0.17 M FPT in pure EDMITFSI.

ionic liquid but cannot solely explain the observed difference. A rough estimate for iR_u of no more than 20 mV can be made with the experimental parameters being used in this work. It should be noted that the ionic conductivity of the pure ionic liquids is smaller than that of the 1 M Et_4NBF_4/acetonitrile solution. Specific conductivities in the range of 3.2 and 6.6 mS/cm were reported for EDMITFSI and DEMITFSI[15] in comparison to 43 mS/cm for 1 M Et_4NBF_4/acetonitrile.[31]

It should be mentioned that a negative limit of −2.1 V should not be exceeded, otherwise no n-dedoping wave is observed. This is due to the fact that the n-doping wave overlaps with the onset of irreversible degradation of the ionic liquid.[15] In the case of the PFPT film grown and cycled in pure DEMITFSI, the cyclic voltammogram of Figure 3 (curve —) exhibits an anodic peak at slightly more positive potential (0.88 V) than when EDMITFSI is used. Hence, the effect of the cations is observed despite that the $TFSI^-$ anions should be mostly involved in the charge compensation of as-grown PFPT and during the redox cycling in the p-doped state. Clearly, the charge compensation mechanism is more complex and perhaps might

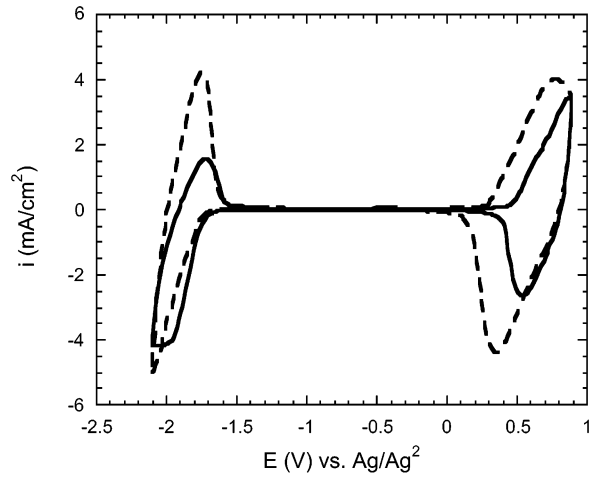

Figure 3. Cyclic voltammogram of a PFPT thin film on a Pt disk electrode in pure EDMITFSI (− − −) and DEMITFSI (—) at a scan rate of 100 mV/s. Growth conditions: Current density = 12.7 mA/cm^2; Deposited charge = 200 mC/cm^2; Deposition solution: 0.17 M FPT in pure ionic liquid. The same ionic liquid was used for the electropolymerization and for recording the cyclic voltammogram.

involve cationic species. Despite these differences and limitations, an electroactive PFPT film electrode can be clearly grown and cycled in neat ionic liquid. This is in agreement with previous reports dealing with polypyrrole in chloroaluminate melts.[5,6] However, the kinetics of switching of this polypyrrole film was reportedly faster in the molten salt than in a conventional acetonitrile-based solution. The difference was explained by higher porosity and a loss of permselectivity of the polymer in the ionic liquid. On the contrary, our data, which suggest slower kinetics in ionic liquids, are in agreement with the more compact polymer as observed by SEM photomicrographs (see Figure 2).

It is also interesting to compare the voltammetric charge (evaluated by integration of the voltammetric waves) and the doping level (charge being stored by repeated monomer unit) of PFPT, grown from pure ionic liquid solution when cycled in ionic liquid and in Et_4NBF_4/acetonitrile (Table 1). The voltammetric charge and the doping levels are comparable in some instances, but some noticeable differences can be observed. The observation of similar doping levels is surprising because higher values were expected in Et_4NBF_4/acetonitrile owing to an expected better swelling of the polymer in the presence of acetonitrile as solvent. The lower n-doping level in EDMITFSI and p-doping level in DEMITFSI stems primarily from the potential limit that was selected for the cyclic voltammetry experiment that does not allow for the complete redox switching of the polymer. As indicated above, this is related to the slower ion transport kinetics and poorer swelling of the polymer in the presence of the ionic liquid that translates into a shift of the anodic wave, poor reversibility of the n-doping process, and poorer cyclability (see below). On the other hand and as expected, it will be shown below that faster kinetics were observed for a thinner PFPT film electrode.

The cyclability of PFPT in pure ionic liquid was investigated by cyclic voltammetry at 100 mV/s over the complete range of electroactivity of both the n- and p-doped states of the polymer. A rapid loss of electroactivity was observed, and more than 75% of the initial voltammetric charge was lost after only 50 cycles. In this case, the deswelling (loss of ionic liquid from the film) of the PFPT film in pure ionic liquid upon cycling leads to a loss of electroactivity. In comparison, the loss of voltammetric charge over 50 cycles is negligible in Et_4NBF_4/acetonitrile. Swelling of the polymer is required to allow facile and fast transport of ionic species in and out of the polymer during its potential cycling. As mentioned above, anion ingress is occurring during p-doping and expulsion during p-dedoping, and alternately, cations are inserted upon n-doping and expulsed upon p-dedoping. In the case of the ionic liquid, the loss of electroactivity could be also due to ion trapping during the dedoping process. This phenomenon is suggested by the data of Figure 3 and Table 1 that demonstrates a significant charge imbalance between the n-doping and n-dedoping charges for the DEMITFSI ionic liquid. Interestingly, a PFPT film subjected to potential cycling in the n-doped region in pure ionic liquid can be reactivated by potential cycling in the p-doped region in the same medium. The first cycle is then characterized by an intense p-doping wave that decayed on the second scan to about 10−20% of the very initial ones (e.g., before the 50 cycles). In addition, an increase of the voltammetric charge is also observed when such PFPT electrode is transferred to a 1 M Et_4NBF_4/acetonitrile solution. These results provide strong evidence that deswelling causes a decrease of electroactivity in the ionic liquid.

Electrochemical Impedance Spectroscopy, EIS. Complex plane impedance plots for the PFPT-coated platinum electrode in pure EDMITFSI are shown in Figure 4 for the p- and n-doping states. Impedance plots for electrode potentials of 0.8 and 0.9 V are characterized by a high frequency straight line with a 45° angle (Warburg-type region) and a nearly vertical line (90°) at low frequency. A similar impedance plot was recorded for PFPT at −1.7 V and is in agreement with those reported for conducting polymers in their conducting (either p- or n-doped) states. On the other hand, at a more negative potential (e.g., −2.1 V), a semicircle appeared at high frequencies in addition to the features mentioned above at lower frequencies. This high-frequency semicircle indicates that an interfacial charge-transfer process has become slow.[32−35] The same trend was observed with PFPT-coated platinum electrodes in the other pure ionic liquid, DEMITFSI.

The low-frequency capacitance of the polymer electrode can be evaluated from the impedance data from the slope of a plot of the imaginary component of the impedance, at low frequency, as a function of the reciprocal of the frequency[21,22,34−36] and are presented in Table 2. The capacitance values are similar for EDMITFSI and DEMITFSI and are in the average of 15 mF/cm^2. These values compare well with those previously reported for PFPT in acetonitrile-based electrolyte[22] and for other conducting polymers.[37]

The high-frequency real axis intercept, R_{high}, the low-frequency limiting real impedance, R_{low} (in the absence of a high-frequency semicircle), and the solution resistance, R_s, were evaluated and used for the determination of the ionic, R_{ion}, and electronic, R_e, resistances with the corresponding equations (1 and 2) of the transmission line model:[21,33]

$$\frac{1}{R_{high} - R_s} = \frac{1}{R_e} + \frac{1}{R_{ion}} \quad (1)$$

$$3(R_{low} - R_s) = R_{ion} + R_e \quad (2)$$

The electronic and ionic conductivities extracted from the impedance data are included in Table 2 for the PFPT-coated in platinum in EDMITFSI and DEMITFSI. Table 2 clearly indicates higher ionic conductivities for the p-doped state relative to the n-doped PFPT. A similar difference has been already observed for other polythiophene derivatives.[21,22] This is attributed to the slower transport of cations ($EDMI^+$ and $DEMI^+$)

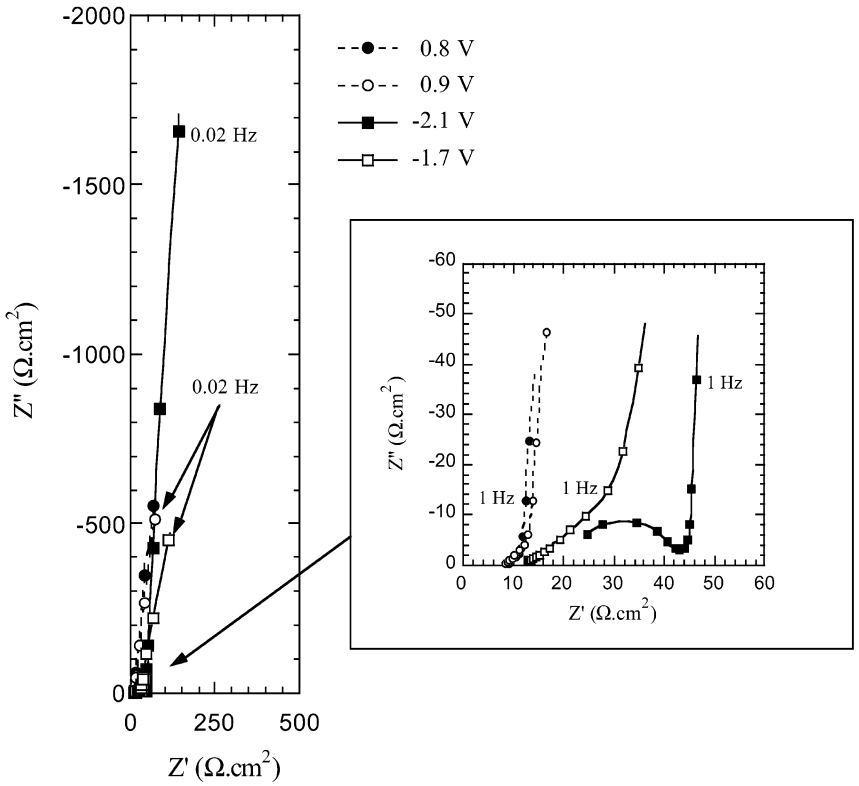

Figure 4. Complex plane impedance plots for PFPT films grown on platinum electrode in pure EDMITFSI ionic liquid at various electrode potentials. Deposited charge = 200 mC/cm^2.

TABLE 2: Electrochemical Impedance Spectroscopy Parameters for PFPT in Pure Ionic Liquids

	EDMITFSI[a] (Rs = 6.5 Ω.cm^2)			DEMITFSI[a] (Rs = 8.0 (Ω.cm^2)		
electrode potential (V vs Ag/Ag$^+$)	low-frequency capacitance C_{LF} (mF/cm^2)	ionic[b] conductivity σ_I(μS/cm) linear transmission line model	electronic[b] conductivity σ_e(μS/cm) linear transmission line model	low-frequency capacitance C_{LF} (mF/cm^2)	ionic[b] conductivity σ_I(μS/cm) linear transmission line model	electronic[b] conductivity σ_e(μS/cm) linear transmission line model
−2.0	13.8	26	170	14.3	26	146
−1.9	18.9	25	161	18.9	23	147
−1.8	4.5	9.0	127	6.5	8.3	124
−0.7	15.8	12	392	13.9	12	370
−0.8	17.2	36	476	14.4	39	400
−0.9	14.6	42	526	15.7	40	408

[a] Growth conditions of PFPT: Deposited charge 200 mC/cm^2, thickness = 20 μm, 0.17 M FPT, and i = 12.7 mA/cm^2. [b] $(R_{High} - R_s)^{-1} = R_E^{-1} + R_I^{-1}$ and $(R_{Low} - R_s) = R_E + R_I$ with R_{High} = Warburg diffusion line intercept with the real impedance axis.

during the n-doping process relative to the anion $(CF_3SO_2)_2N^-$) in the p-doped polymer. Furthermore, these ionic conductivities for the p-doped state (∼40 μS/cm) are lower than those previously reported for PFPT in 0.2 M Et_4NBF_4/acetonitrile (180 μS/cm by using a thickness of 2 μm).[21] In this case, the conductivity of the 0.2 M Et_4NBF_4/acetonitrile solution is 12 mS/cm.[31] This seems to demonstrate a slower transport of anions ($(CF_3SO_2)_2N^-$) and cations ($EDMI^+$ and $DEMI^+$) in the polymer in the presence of the ionic liquids as electrolyte compared to the Et_4NBF_4/acetonitrile electrolyte. This might be due to the more compact film generated in the ionic liquid. In addition, the lower conductivity of the ionic liquid relative to the acetonitrile-based electrolyte also contributes to these lower values because it was previously demonstrated that the ionic conductivity of a conducting polymer is proportional to the solution conductivity.[38] The ratios of the ionic conductivities for the solutions are 0.27 or 0.55 (3.2 (6.6) mS/cm/12 mS/cm), but that of the ionic conductivities of the polymer is 0.14 (26 μS/cm /180 μS/cm). The lower ratio for polymer conductivities implies that the films are less porous in the ionic liquid. On the other hand, Table 2 shows a higher electronic conductivity for p-doped PFPT relative to the n-doped state but no significant difference between the two ionic liquids. In a previous study with PFPT with acetonitrile as solvent, the limiting case for a highly conducting state with $R_e <<< R_I$ was considered and only the ionic resistance was computed.[21,22] However, the impedance data for PFPT in ionic liquids show a shift of the high frequency intercept (between 0.7 and 0.9 V and −1.8 and −2 V) that is consistent with a variation of both the electronic and ionic resistances. Nevertheless, some caution is needed for the analysis of these R_e and R_I values because they are subjected to significant uncertainty which is linked to the solution resistance values that were used for the calculation. This was clearly demonstrated in a recent study with another polythiophene derivative.[35] Nonetheless, the higher conductivity for the p-doped state relative to the n-doped form is in agreement with literature data and will be confirmed below by the in situ conductivity measurements.

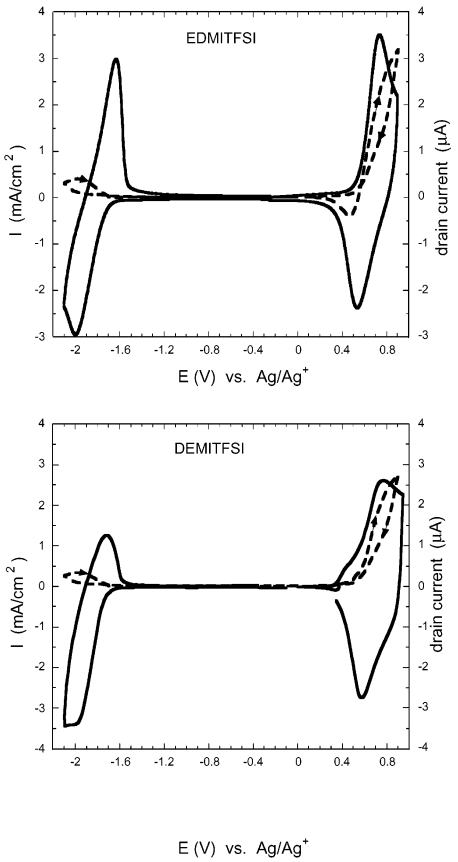

Figure 5. Variation of the drain current, I_d, with the electrode potential for a PFPT film electrode in pure ionic liquids. The drain voltage was set at 25 mV. The cyclic voltammogram and the I_d-potential curve were recorded at a scan rate of 5 mV/s. Deposited charge = 1.3 mC/cm^2 at a current density of 5.2 mA/cm^2.

In situ conductivity measurements of PFPT films (deposited charge 1.3 mC/cm^2) were performed in the pure ionic liquids. Figure 5 reports the variation of the drain current, I_D (which is proportional to the electronic conductivity), as a function of electrode potential together with the corresponding cyclic voltammograms. First, the cyclic voltammograms are similar to those reported above in Figure 2 but a smaller peak potential separation is observed because of the thinner polymer films and the slower scan rate. Second, the I_D-E curves are characterized by a sigmoidal shape, and an increase of I_D occurs at the onset of doping processes; the latter is indicated by the increase of the current of the cyclic voltammogram. The drain current or the electronic conductivity for the p-doped state is about an order of magnitude higher than for the n-doped state. The trend is in qualitative agreement with the impedance data, albeit the ratio between the electronic conductivity of the p- and n-doped states computed from the I_D-E data is somewhat higher. Finally, the electronic conductivity in the presence of Et_4NBF_4/acetonitrile[39] is also slightly higher than with the ionic liquids.

X-ray Photoelectron Spectroscopy, XPS. XPS is a powerful tool to characterize the electronic properties of conducting polymers and the chemical (ionic) surface composition of conducting polymers. In this work, XPS was used to characterize as-grown PFPT and PFPT in both the p- and n-doped states when a pure ionic liquid was used as electrolyte. The XPS survey spectrum (Supporting Information) of the as-grown PFPT shows the characteristic C 1s (285 eV), S 2p (165 eV), S 2s (230 eV), and F 1s (685 eV) peaks of the polythiophene derivative. The as-grown polymer is obtained in the oxidized (p-doped) state and the expected presence of $TFSI^-$ as dopant

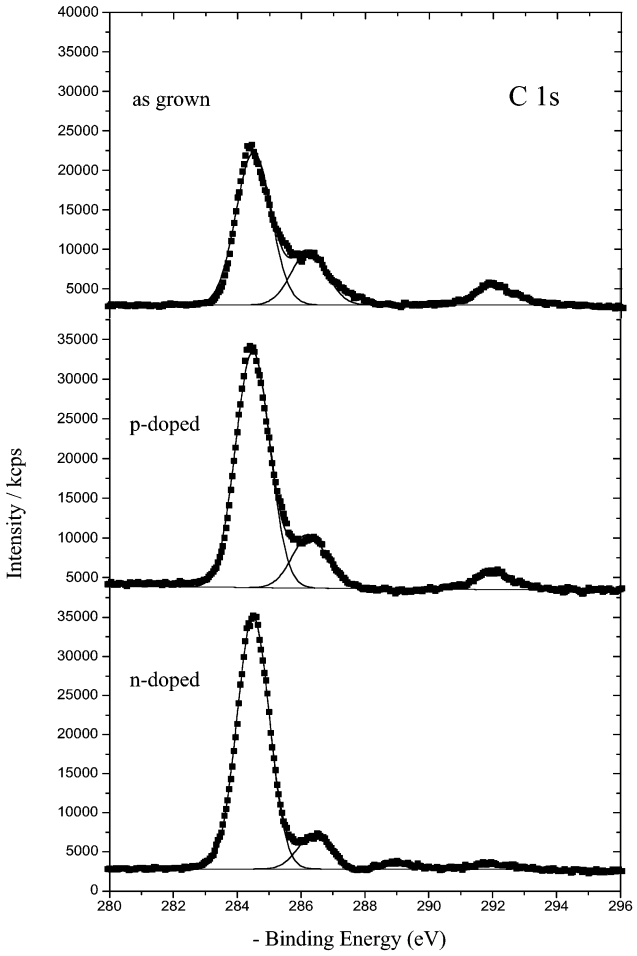

Figure 6. XPS C 1s core level spectra of PFPT films: (a) as grown, (b) oxidized at 0.8 V in the p-doped state, and (c) reduced at −2.07 V in the n-doped state.

gives rise to the N 1s peak at 400 eV and these anionic species contribute also to the S 2p, S 2s, and F 1s peaks. Similar spectra were recorded for PFPT in the p- and n-doped states although some differences are evident. These differences will be more clearly detected and analyzed further with the aid of the core level spectra below.

Figures 6−9 depict the C 1s, F 1s, N 1s, and S 2p core level spectra, respectively, for the as-grown PFPT and both the p- and n-doped polymers. The spectra for the as-grown and the p-doped PFPT are very similar but differ significantly from those of the n-doped polymer. These spectra are complicated by the presence of common atoms in both the polymer backbone and the cationic and anionic species of the ionic liquid. For example, N is found in both ionic species, whereas F is present in the polymer and the anions. In addition, some residual ionic liquid is always present despite the fact that the polymer electrode is thoroughly rinsed with dichloromethane. Nonetheless, it will be demonstrated below that a careful analysis of the XPS data allow for the determination of the surface composition of the PFPT electrode. A qualitative description of the core level spectra will be initially presented and will be followed by a more quantitative analysis of the data. Information concerning the deconvolution results can be found in the Supporting Information.

The C 1s core level spectra show the characteristic C 1s peak at 284.5 eV, a second peak at 286.3 eV, and a third one at 292.0 eV (Figure 6). The latter is clearly observed for the as-grown and the p-doped polymers and is attributed to the carbon atoms

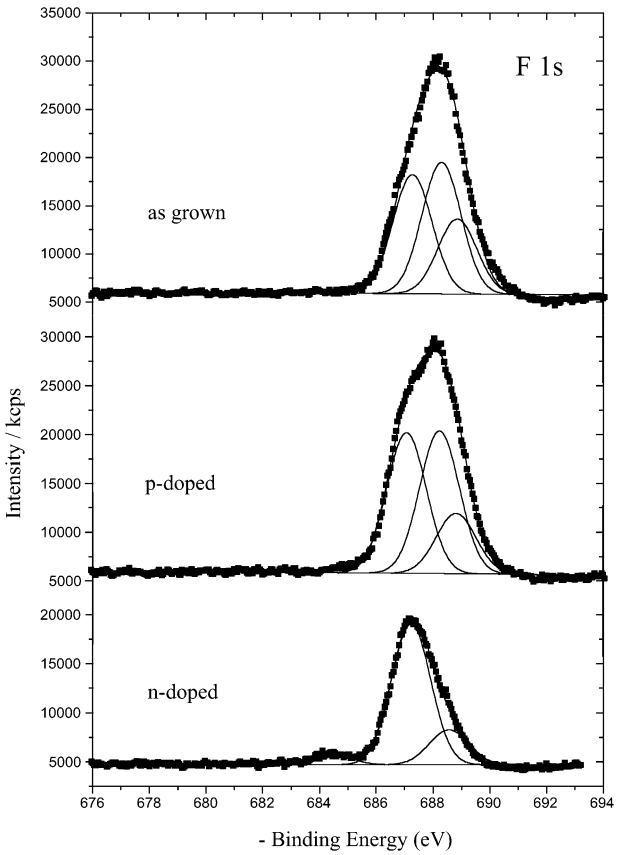

Figure 7. XPS F 1s core level spectra of PFPT films: (a) as grown, (b) oxidized at 0.8 V in the p-doped state, and (c) reduced at −2.07 V in the n-doped state.

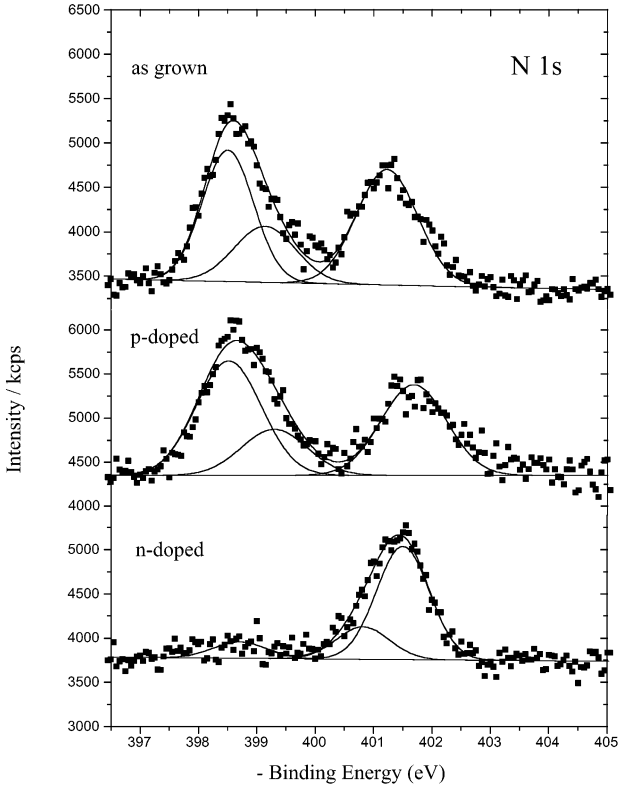

Figure 8. XPS N 1s core level spectra of PFPT films: (a) as grown, (b) oxidized at 0.8 V in the p-doped state, and (c) reduced at −2.07 V in the n-doped state.

that are bonded to fluorine of the $TFSI^-$ anions. This is consistent with the fact that $TFSI^-$ anions act as a dopant for the oxidized PFPT.

The F 1s spectra of the as-grown and p-doped PFPT shown in Figure 7 can be fitted with three components that are attributed to the fluorinated polymer at 687.2 eV, the $TFSI^-$ doping anions at 688.2 eV, and to residual ionic liquid (EDMITFSI) at 688.7 eV. The second peak is absent for the n-doped PFPT. Qualitatively, this is consistent with the incorporation of $TFSI^-$ in the p-doped polymer and its expulsion in the n-doped form.

The N 1s spectra show two major peaks that can be deconvoluted with three components (Figure 8). The peak at lower binding energy is related to the $TFSI^-$ anions, and the one at higher binding energy is attributed to the $EDMI^+$ cations. The low binding energy peak requires two components for the as-grown and p-doped polymers, whereas the same is true for the high binding energy peak for the n-doped PFPT. The core level spectra of the as-grown and oxidized PFPT should have only one N 1s component that would be related to the presence of $TFSI^-$ doping anions. The additional pair of peaks for $EDMI^+$ and $TFSI^-$ with a 2:1 ratio (two N in $EDMI^+$ and one N in $TFSI^-$) is explained by the presence of residual ionic liquid in the polymer or at the polymer surface. The N 1s spectrum of the n-doped PFPT also shows a peak at 401.5 eV that is linked to the presence of the $EDMI^+$ doping cations. The presence of some residual ionic liquid in the n-doped film is indicated by the doublet at 398.7 and 400.8 eV. This represents a slight shift to lower binding energies in comparison to the as-grown and oxidized films. A similar shift of the F 1s component of the ionic liquid to lower binding energy was also noticed for the n-doped film. The reasons for this shift are not clear for the moment and require further investigation.

The S 2p core level spectra are characterized by two sets of doublets (Figure 9). The first one at low binding energy is attributed to the sulfur of the thiophene, whereas the one at higher binding energy represents the contribution of the $TFSI^-$ anions. In the case of the n-doped PFPT, the high binding energy component is very weak in agreement with an absence of $TFSI^-$ anions in the n-doped material except for some residual ionic liquid. First, the low binding energy envelope can be fitted with two pairs of doublets. In the case of the as-grown and p-doped PFPT, a low binding energy doublet with binding energies of 163.5 and 164.6 eV with a 2:1 ratio is attributed to the neutral sulfur atoms of PFPT. A second doublet at 165.3 and 166.2 eV is assigned to the oxidized sulfur. In the case of the n-doped PFPT, the later is not observed, but instead, a low binding energy doublet with binding energies of 162.6 and 163.3 eV is detected. This doublet is attributed to negatively charged sulfur atoms of the n-doped polymer. A similar doublet for negatively charged sulfur atoms was recently observed for polycyclopenta[2,1-b;3,4-b′]dithiophen-4-one, PCDT,[35] and PFPT[39] when these polythiophene derivatives where reduced in Et_4NBF_4/acetonitrile. However, in the latter cases, the low binding energy components were observed at lower values (160.1 and 161.4 eV). The difference might be attributed to a spontaneous dedoping[40] of PFPT in ionic liquids. Alternatively, it seems more plausible to assume that the interaction between the negatively charged and solvated polymer with solvated cations differs from those between the polymer and the cations in the ionic liquid. Indeed, the higher charge delocalization on the $DEMI^+$ and $EDMI^+$ cations should give rise to a S 2p doublet at slightly higher binding energies as compared with the Et_4N^+ cations. Second, the S 2p component at higher binding energy can be fitted into two pairs of doublets; the one at lower binding energies (S $2p_{3/2}$

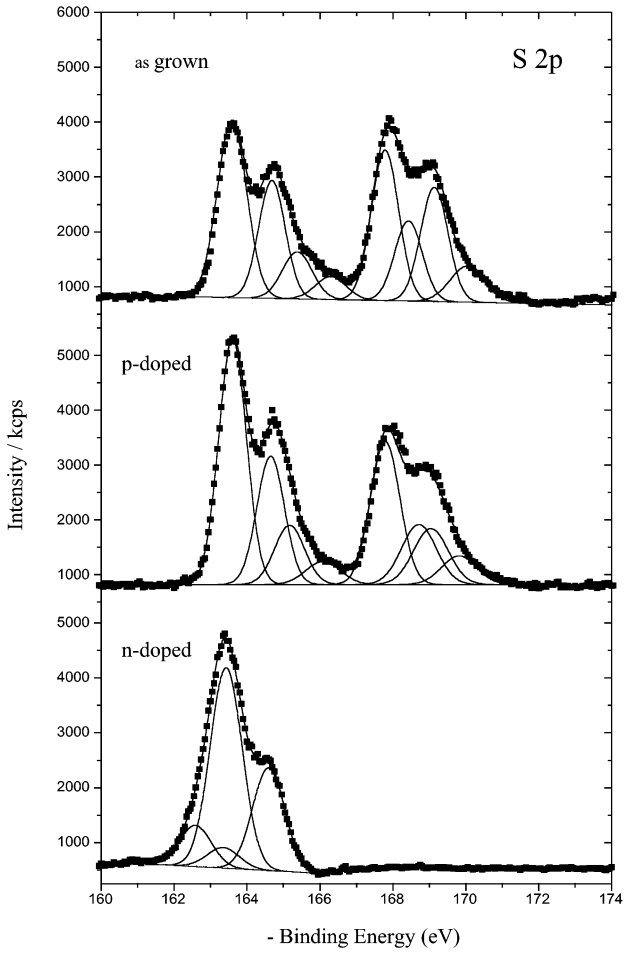

Figure 9. XPS S 2p core level spectra of PFPT films: (a) as grown, (b) oxidized at 0.8 V in the p-doped state, and (c) reduced at −2.07 V in the n-doped state.

TABLE 3: Doping Level Deduced from the XPS Data

doping level, x			
as grown	p-doped	n-doped	
0.20	0.20		$(S\ 2p)_{PFPT}{}^{+}/(S\ 2p)_{PFPT}$
0.29	0.24		$(S\ 2p)_{TFSI}{}^{-}/(S\ 2p)_{PFPT}$
		0.08	$(S\ 2p)_{PFPT}{}^{-}/(S\ 2p)_{PFPT}$
0.28	0.21		$(N1s)_{TFSI}{}^{-}/(S\ 2p)_{PFPT}$
		0.09	$(N1s)_{EDMI}{}^{+}/(S\ 2p)_{PFPT}$
0.23	0.20		$(F1s)_{TFSI}{}^{-}/(F1s)_{PFPT}$
		0.07	$(N1s)_{EDMI}{}^{+}/(F1s)_{PFPT}$

at 169.1 eV and S $2p_{1/2}$ at 169.9 eV) is attributed to the $TFSI^-$ dopant anions and that at higher energy is related to the $TFSI^-$ anions of the residual ionic liquid.

The surface doping level of the polymers can be evaluated with the XPS data[39,41,42] and are given in Table 3. The doping level of the as-grown and oxidized PFPT is about 0.2, whereas that of the n-doped PFPT is smaller at about 0.1. The doping level can be obtained from the positively or negatively charged fraction of the S 2p envelope of the thiophene units (e.g., low binding energy peak). For example, in the case of the p-doped PFPT, values of 0.2 and 0.24 are obtained with the S 2p data by taking the $S_{PFPT}{}^{+}/S_{PFPT}$ and $S_{TFSI}\text{-}/S_{PFPT}$ ratios, respectively. In addition, the presence of different atoms in the dopant ions provide alternative ways for the evaluation of the doping level. Table 3 shows that the various approaches that have been used to evaluate the doping level yielded similar values with one exception for the as-grown polymer. For the p-doped PFPT, the doping level can be obtained from the N 1s/S 2p ratio (0.21) by taking the ratio of the N 1s contribution of the $TFSI^-$ dopant and the total S 2p envelope of PFPT. The ratio of the F 1s component of the $TFSI^-$ dopant to that of the F 1s component of PFPT also yields the doping level (0.20 in Table 3) by assuming the presence of six fluorine atoms for the anions. In the case of the n-doped PFPT, the agreement between the various methods is very good. These doping levels are determined from the appropriate ratios of the contributions of the negatively charged S 2p fraction of PFPT and total PFPT contribution to the S 2p envelope and that of the N 1s of $EDMI^+$ and F 1s of PFPT.

The presence of residual ionic liquid in the films was confirmed by the XPS data. Previous studies have shown that as-grown and electrochemically cycled conducting polymers may contain a high concentration of additional electrolyte.[43] Presumably, the same phenomenon can occur for PFPT cycled in ionic liquids, but the extent of salt inclusion arising solely from a similar mechanism is difficult to asses because of the viscous nature of the ionic liquid which makes it difficult to remove completely from the polymer surface by rinsing.

Conclusion

It is clear from the data presented here that PFPT can be grown and cycled in pure ionic liquids. The electrochemical behavior reported here is very similar to that observed in common nonaqueous electrolyte (e.g., tetraalkylammonium salt in acetonitrile). However, the kinetics of the redox processes are slighlty slower, and the polymer is less stable upon repeated potential cycling. These differences are attributed to a less swollen PFPT film in ionic liquids. XPS measurements revealed that the surface composition of PFPT can be modulated by potential cycling. The oxidized PFPT is charge compensated by anions of the ionic liquid, whereas the n-doped form is neutralized by cations of the ionic liquid. This is in agreement with the accepted model of conducting polymer doping. However, the XPS analysis is complicated by the fact that it is difficult to remove excess ionic liquid from the film surface by rinsing because of their high viscosity and low vapor pressure.

Acknowledgment. This research was funded by the Natural Science and Engineering Research Council of Canada through a strategic grant (to L.B. and D.B.) and an equipment grant for an XPS spectrometer (to D.B. and nine others). The financial contribution of UQAM is also acknowledged. We thank R.Mineau from UQAM (Département des Sciences de la Terre) for the SEM analysis and Dominique Villers for the help in some experiments. E.N. acknowledged the "Département de Chimie de l'UQAM" for a fellowship.

Supporting Information Available: X-ray photoelectron spectroscopy survey and deconvoluted C1s, F1s, N1s, S2p, core level spectra for as-grown, p-doped, and n-doped PFPT; deconvolution parameters of the core levels spectra and ionic conductivity data for Et_4NBF_4 /acetonitrile solutions. This material is available free of charge via the Internet at http://pubs.acs.org.

References and Notes

(1) *Handbook of Conducting Polymers*, 2nd ed.; Skotheim, T.; Elsembaumer, R. L.; Reynolds, J. R.; Marcel Dekker: New York, 1998.

(2) *Handbook of Organic Conducting Molecules and Polymers: Transport, Photophysics and Applications*; Nalwa, H. S.; Wiley: New York, 1998; Vol. 4.

(3) Roncali, J. *J. Mater. Chem.* **1999**, *9*, 1875.

(4) Geniès, E. M.; Lapkowski, M.; Tsintavis, C. *New. J. Chem.* **1988**, *12*, 181.

(5) Pickup, P. G.; Osteryoung, R. A. *J. Electroanal. Chem.* **1985**, *195*, 323.
(6) Pickup, P. G.; Osteryoung, R. A. *J. Am. Chem. Soc.* **1984**, *106*, 2294.
(7) Huddleston, J. G.; Willauer, H. D.; Swatloski, R. P.; Visser, A. E.; Rogers, R. D. *J. Chem. Soc., Chem. Commun.* **1998**, 1765.
(8) Kelley, C. S.; Carlin, R. T. *J. Electrochem. Soc.* **1993**, *140*, 1607.
(9) Yu, C. L.; Winnick, J.; Kohl, P. A. *J. Electrochem. Soc.* **1991**, *139*, 699.
(10) Fung, Y. S.; Chau, S. M. *J. Appl. Electrochem.* **1993**, *23*, 346.
(11) Fuller, J.; Carlin, R. T.; De Long, H. C.; Haworth, D. *J. Chem. Soc., Chem. Commun.* **1994**, 299.
(12) Earle, M. J.; McCormac, P. M.; Seddon, K. R. *J. Chem. Soc., Chem. Commun.* 1998, 2245.
(13) Adams, C. J.; Earle, M. J.; Roberts, G.; Seddon, K. R. *J. Chem. Soc., Chem. Commun.* **1998**, 2097.
(14) Welton, T. *Chem. Rev.* **1999**, *99*, 2071.
(15) Bonhôte, P.; Dias, A.-P.; Papageorgiou, N.; Kalyanasundaram, K.; Grätzel, M. *Inorg. Chem.* **1996**, *35*, 1168.
(16) McEwen, A. B.; Ngo, H. L.; LeCompte, K.; Goldman, J. L. *J. Electrochem. Soc.* **1999**, *146*, 1687.
(17) Sarker, H.; Gofer, Y.; Killiam, J. G.; Poehler, T. O.; Searson, P. C. *Synth. Met.* **1999**, *88*, 179.
(18) Gofer, Y.; Killiam, J. G.; Sarkeer, H.; Poehler, T. O.; Searson, P. C. *J. Electroanal. Chem.* **1998**, *443*, 103.
(19) Killiam, J. G.; Gofer, Y.; Sarker, H.; Poehler, T. O.; Searson, P. C. *Chem. Mater.* **1999**, *11*, 1075.
(20) Sarker, H.; Gofer, Y.; Killian, J. G.; Poehler, T. O.; Searson, P. C. *Synth. Met.* **1998**, *97*, 1.
(21) Guerrero, D. J.; Ren, X.; Ferraris, J. P. *Chem. Mater.* **1994**, *6*, 1437.
(22) Ferraris, J. P.; Eissa, M. M.; Brotherston, I. D.; Loveday, D. C.; Moxey, A. A. *J. Electroanal. Chem.* **1998**, *459*, 57.
(23) Laforgue, A.; Simon, P.; Fauvarque, J. F. J. *Power Sources* **1999**, *80*, 142.
(24) Ferraris, J. P.; Eissa, M. M.; Brotherston, I. D.; Loveday, D. C. *Chem. Mater.* **1998**, *10*, 3528.
(25) Soudan, P.; Lucas, P.; Breau, L.; Bélanger, D. *Langmuir* **2000**, *16*, 4362.
(26) Lucas, P.; Mehdi, N. El.; Ho, H. A.; Bélanger, D.; Breau, L. *Synthesis* **2000**, *9*, 1253.
(27) Bartelt, J. E.; Deakin, M. R.; Amatore, C.; Wightman, R. M. *Anal. Chem.* **1988**, *60*, 2167.
(28) Schiavon, G.; Sitran, S.; Zotti, G. *Synth. Met.* **1989**, *32*, 209.
(29) Zotti, G. *Synth. Met.* **1998**, *97*, 267.
(30) McCoy, C. H.; Lorkovic, I. M.; Wrighton, M. S. *J. Am. Chem. Soc.* **1995**, *117*, 6934.
(31) The conductivity measurements were performed by electrochemical impedance spectroscopy (see the Supporting Information).
(32) Albery, W. J.; Elliott, C. M.; Mount, A. R. *J. Electroanal. Chem.* **1990**, *15*, 288.
(33) Pickup, P. G. *J. Chem. Soc., Faraday Trans.* **1994**, *90*, 1115.
(34) Ren, X.; Pickup, P. G. *J. Electroanal. Chem.* **1997**, *420*, 251.
(35) Fusalba, F.; El Mehdi, N.; Breau, L.; Bélanger, D. *Chem. Mater.* **1999**, *11*, 2743.
(36) Fusalba, F.; Ho, H. A.; Breau, L.; Bélanger, D. *Chem. Mater.* **2000**, *12*, 2581.
(37) Garcia, B.; Fusalba, F.; Bélanger, D. *Can. J. Chem.* **1997**, *75*, 1536.
(38) Ren, X.; Pickup, P. G. *J. Electrochem. Soc.* **1992**, *139*, 2102.
(39) (a) Naudin, E.; Dabo, P.; Guay, D.; Breau, L.; Bélanger, D. *ACS Polym. Mater. Sci. Eng.* (PMSE), **1999**, *80*, 629. (b) Naudin, E.; Dabo, P.; Guay, D.; Bélanger, D. Submitted.
(40) Levi, M. D.; Gofer, Y.; Aurbach, D.; Lapkowski, M.; Vieil, E.; Serose, J. *J. Electrochem. Soc.* **2000**, *147*, 1096.
(41) Fusalba, F.; Bélanger, D. *J. Phys. Chem. B* **1999**, *103*, 9044.
(42) Bach, C. M.; Reynolds, J. R. *J. Phys. Chem.* **1994**, *98*, 13636.
(43) Duffitt, G. L.; Pickup, P. G. *J. Chem. Soc., Faraday Trans.* **1990**, *88*, 1417.